Additive Manufacturing 89 (2024) 104290

Contents lists available at ScienceDirect

Additive Manufacturing

journal homepage: www.elsevier.com/locate/addma

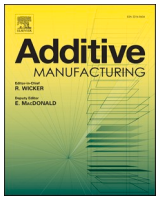

Enhancing melt-processing and 3D printing suitability of polyhydroxybutyrate through compounding with a bioplasticizer derived from the valorization of levulinic acid and glycerol

Elena Togliatti [a,b,1], Luca Lenzi [b,c,1], Micaela Degli Esposti [b,c], Maila Castellano [d], Daniel Milanese [a,c], Corrado Sciancalepore [a,c,*], Davide Morselli [b,c,**], Paola Fabbri [b,c]

[a] Department of Engineering for Systems and Industrial Technologies, Università di Parma, Parco Area delle Scienze 181/A, Parma 43124, Italy
[b] National Interuniversity Consortium of Materials Science and Technology (INSTM), Via Giusti 9, Firenze 50121, Italy
[c] Department of Civil, Chemical, Environmental and Materials Engineering, Università di Bologna, Via Terracini 28, Bologna 40131, Italy
[d] Department of Chemistry and Industrial Chemistry, Università di Genova, Via Dodecaneso 31, Genova 16146, Italy

ARTICLE INFO

Keywords:
PHAs
PHB
Bioplasticizer
Molten state processing
Material extrusion (MEX)

ABSTRACT

In the near future, polyhydroxybutyrate (PHB) may become a valuable widespread alternative to the conventional fossil-based commodity plastics, if drawbacks related to its melt-processability and mechanical properties are overcome. In this work, PHB disadvantages are mitigated by compounding with glycerol trilevulinate (GT) bioplasticizer. The additive synthesis has been studied and optimized, starting from bio-based reagents that are wastes from other productions. GT has shown a remarkable plasticizing effect, making it to compete with commercial green plasticizers, for which several health concerns have recently arisen. The hindrance of GT allowed to increase the free space among the polymeric chains, producing a reduction of the glass transition temperature of PHB of approx. 10 °C with only 5 wt% of additive. The same content of GT also decreases the typical high stiffness of PHB of approx. 30 % and reduces its melt viscosity of 28 %, which are similar or even better plasticization effects that can be obtained with commercial plasticizers. Moreover, GT has made PHB suitable for extrusion to obtain filaments and fabrication of complex architectures by injection-molding and 3D printing, importantly reducing the processing temperature from 200 to 180 °C, thus limiting the associated thermal degradation phenomena. This work opens a new approach based on polymer-compounding to simply mitigate the limiting properties of polyhydroxyalkanoates towards a new class of sustainable commodity plastics.

1. Introduction

The concept of bioeconomy, defined two decades ago, has stimulated an intense development of innovative approaches to address global challenges such as plastic pollution, depletion of fossil resources, and reduction of greenhouse gas emissions [1]. The bioeconomy serves as a link between biotechnology and chemical industries, intending to deliver sustainable products produced by green approaches [2–4]. The polymer industry is also facing a deep transition towards the utilization of renewable resources to replace the most conventional fossil-derived sources [5,6]. In these terms, bioplastics derived from renewable biomass building blocks are considered the most promising alternatives. They offer several benefits, including reduced energy consumption for production, non-toxicity, and environmentally friendly degradation with limited greenhouse gas emissions [3,7]. Various biomass feedstocks, including corn, starch, cellulose, lignin, fats, oils, and organic wastes, are used to produce building blocks that are then converted into the generally so-called biopolymers [8,9]. Among them, polyhydroxyalkanoates (PHAs) represent one of the most promising polymer families to replace some of the plastic commodities. PHAs are bio-based,

* Corresponding author at: Department of Engineering for Systems and Industrial Technologies, Università di Parma, Parco Area delle Scienze 181/A, Parma 43124, Italy.
** Corresponding author at: Department of Civil, Chemical, Environmental and Materials Engineering, Università di Bologna, Via Terracini 28, Bologna 40131, Italy.
E-mail addresses: corrado.sciancalepore@unipr.it (C. Sciancalepore), davide.morselli6@unibo.it (D. Morselli).
[1] Authors contributed equally.

https://doi.org/10.1016/j.addma.2024.104290
Received 4 April 2024; Received in revised form 3 June 2024; Accepted 1 July 2024
Available online 4 July 2024

non-toxic [10], and biodegradable [11] thermoplastic polyesters produced by bacterial fermentation in an aqueous environment [12–14]. Very recent studies have shown that PHAs are not only suitable as replacements for commodities but also for specific advanced applications, including biomedical [15,16], packaging [17,18], electronics [19], membranes for gas separation [20] or water remediation[21], sensors [22] and agricultural [23,24]. Among PHAs, the homopolymer poly (3-hydroxybutyrate) (PHB) has received considerable interest in the last decades [25]. The isotactic and stereoregular structure of PHB results in a high crystallinity degree, which can reach almost 80 % [26], leading to high stiffness, low tensile strength, and elongation at break compared to conventional polyesters. In addition, the widespread use of PHB as a commodity polymer is limited by the narrow temperature range of melt-processability. This is due to its high melting temperature, ranging from 170 to 190 °C depending on the molecular weight [27], which is close to the onset temperature (approx. 200 °C) where irreversible degradation phenomena occur [28]. The limited thermal stability in the molten state hinders the possibility of processing and manufacturing PHB with techniques such as extrusion, injection molding, film blowing, or additive manufacturing [29,30].

In the near future, PHB might become a viable alternative to conventional commodity polymers if its limited processability and mechanical properties are overcome. The most straightforward strategy to simultaneously tailor its mechanical properties and melt-processability is based on compounding PHB with a suitable plasticizer[31]. The combination of biodegradable polymers with petroleum-based plasticizers, like phthalates, raises concerns about potential alterations to biodegradability, biocompatibility, and the bio-based origin of the polymer [32]. Furthermore, these plasticizers are released into the environment during polymer biodegradation, posing a risk to the ecosystems [33].

A more sustainable alternative is represented by the so-called “green plasticizers”, which market is rapidly growing [34] due to the increased awareness of the harmful effects of traditional plasticizers [35]. Several green additives have been proposed starting from natural resources like vegetable oils, fatty acids, and lignocellulosic biomasses [36–39]. Nevertheless, green plasticizers still present several drawbacks compared to traditional plasticizers such as high production cost [40], low plasticizing efficiency [41], high leachability [41,42], and low versatility towards different polymers [41,43]. Recently, two well-known commercial green plasticizers, the 1,2-cyclohexane dicarboxylic acid diisononyl ester (DINCH) and acetyl tributyl citrate (ATBC), have also raised lots of concerns [44,45]. Many researchers have been discussing DINCH safety, demonstrating how its exposure has a direct impact on biological systems [44,46,47]. Regarding ATBC, it has been reported that this additive results in a potential endocrine disruptor, is neurotoxic, and can increase body fat content as observed by *in vivo* animal experiments [45,48,49]. The combination of these factors with its high leachability [50,51] has been increasing the concerns regarding the ATBC as a safe plasticizer. Using the green principles [52], it is possible to design a biodegradable and non-harmful plasticizer, which can be used to enhance mechanical properties and melt-processability of PHB, but with a controlled environmental impact.

Lately, the use of additive manufacturing (AM) approaches has been explored for PHAs in the biomedical sector [53], such as drug delivery systems [54,55], or patient-specific scaffolds for bone and tissue regeneration [56,57]. Fused Deposition Modelling (FDM) is still underutilized for PHAs [58], compared to electrospinning [59–61] and selective laser sintering [62] due to the complex melt rheology of this polymer family. The fabrication of PHB filaments for FDM by the addition of sustainable plasticizers is still very limited. Until now the PHAs processability has been improved by blending them with polylactic acid (PLA) [63] or adding fossil-based plasticizers for both extrusion and 3D printing[64,65]. In these regards, the existing green alternatives have not completely replaced the use of fossil-based plasticizers, which have been instead experiencing an increasing demand [66]. Indeed, only a few studies have investigated the use of green plasticizers to tune PHAs properties and processability [37,67,68].

In this study, we propose the production of PHB compounds using glycerol trilevulinate (GT) as bioplasticizer to overcome the aforementioned disadvantages of PHB. The carboxylic groups-rich structure and high hindrance of GT make this molecule specifically designed for plasticizing polyesters as PHB and obtaining compounds with long-lasting properties [69]. GT has been produced through a green approach based on a solvent-free esterification valorizing bio-based levulinic acid (LA) and glycerol (GLY). The properties of the plasticized PHB compounds have been investigated in relation to their processability by using extrusion (Ex), injection molding (IM), and FDM with the aim of producing controlled-porosity scaffolds that can potentially find application in bone tissue regeneration. Furthermore, the plasticization effect and processability of PHB/GT compounds (in various ratios) have been compared with DINCH and ATBC as representative commercial green plasticizers, aiming at determining the effectiveness of GT as a sustainable alternative and assessing its potential use in industrial applications.

2. Main (results and discussion)

The Scheme 1 illustrates the flowchart followed in this study. Initially, our focus has been the optimization and upscaling of the synthesis of the GT bioplasticizer, which has been previously designed for biopolyesters [69]. In detail, the synthesis has been based on the acid-catalyzed esterification of LA with GLY by a mild-conditions and solvent-free approach. Subsequently, PHB has been compounded with GT in various ratios and thermal, mechanical, and rheological properties of the compounds have been characterized. Thanks to the collected data, PHB/GT compounds have been processed in molten state using semi-industrial equipment (Ex, IM, and FDM), overcoming the known challenges associated with the melt-processability of this biopolyester. Characterization and processing tests have resulted in the fine tuning of equipment parameters and ultimately enabling the fabrication of plasticized PHB samples with complex geometry by 3D printing.

To optimize and scaleup the GT synthesis [69], reaction parameters such as temperature (110 °C), reagent molar ratio (LA/GLY = 5), and catalyst amount have been kept constant, whereas the influence of time on the yield has been studied. The progress of the reaction has been investigated through Fourier Transform Infra-Red spectroscopy (FT-IR) for 24 h, analyzing the reaction mixture during the first 8 h and from the 16th to the 24th hour (Fig. 1A). During the progression of the reaction, the distinct peak between 3600 and 3000 cm^{-1}, corresponding to the hydroxyl groups of the reactants, has been observed to decrease over time (Fig. 1B). However, the expected disappearance of the peak at the complete consumption of the reagents was not observed due to the excess of LA. Indeed, the OH groups responsible for the signal, shown in Fig. 1B, were still present even after 24 h of reaction. The progression of the reaction has been investigated by monitoring the peaks at 1733 and 1713 cm^{-1}, ascribable to the stretching of the ketonic groups of the LA moieties and to the ester bonds formed during the esterification reaction between GLY and LA, respectively. The transmittance of the peak at 1713 cm^{-1} remained constant for the whole duration of the reaction when no undesired ketalization reaction takes place [69], while the intensity of the ester signal at 1733 cm^{-1} kept on increasing with the formation of GT (Fig. 1B). The ratio between the intensity of the two peaks, calculated by Eq. (1) (details in the Section 4), has been used as an indication of the reaction progress (Fig. 1C), by fitting the experimental data (by modified Hill function with offset) to determine the reaction kinetic. The fitting curve has revealed that the ratio between the two peaks did not show any significant variation after 16 hours, suggesting that the esterification reached the equilibrium. By quenching the reaction after 16 hours, a yellowish viscous liquid was obtained with an 82 % molar yield. The final structure of GT was confirmed by ^{1}H NMR analysis reported in Figure S1. Furthermore, the

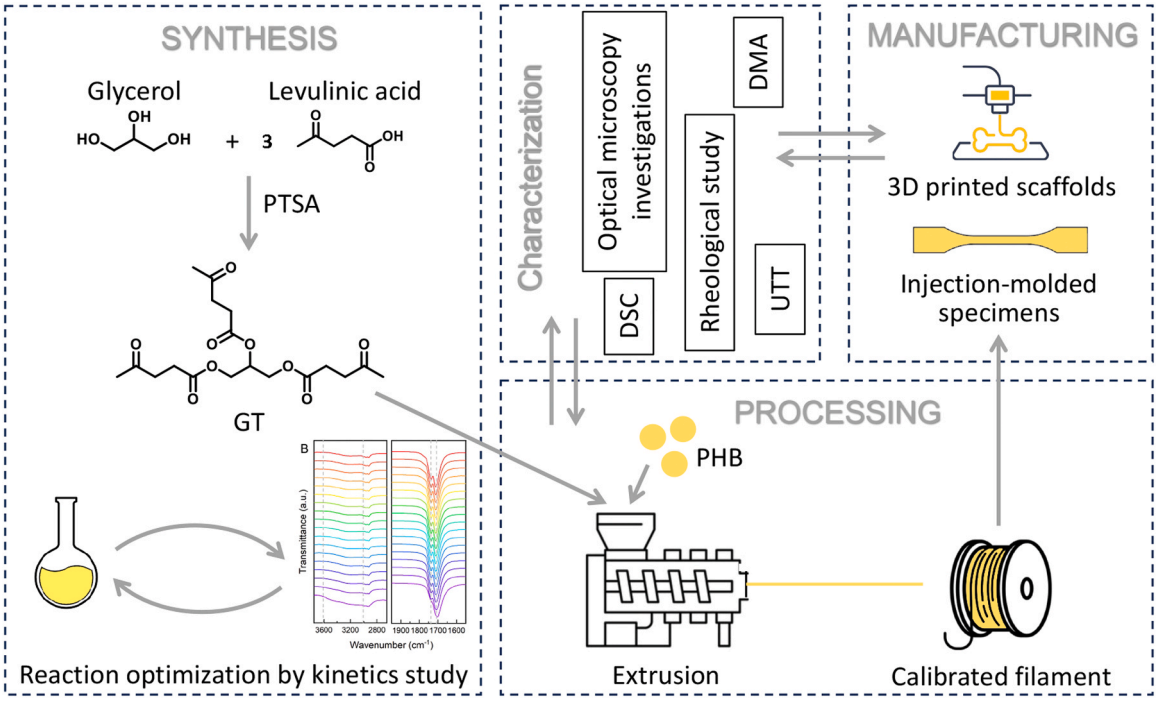

Scheme 1. Schematic representation of the flowchart used for the study.

esterification has been scaled up from an initial production of approximately 7 g [69] per batch of GT up to 17 g.

Solvent-mediated techniques are commonly used for preparing polymeric formulations and samples at a laboratory scale [70]. Specifically, for PHB the most frequently used solvents are chloroform ($CHCl_3$) [71,72] or dichloromethane (CH_2Cl_2) [73,74], both of which are well-known toxic substances. Although solvent-mediate processing may be a simple approach at initial research stage, it can become difficult to scale it up at an industrial scale especially if large amounts of toxic solvents are involved in the process. On the other hand, melt-processing allows to avoid the use of toxic chemicals and to have a larger production rate using equipment that closely resembles industrial machineries.

Twin screw extrusion is the most traditional processing technique to obtain homogeneous mixing of multi-component polymer-based composites [75–77]. The melt-processability of PHB by extrusion is rather difficult mainly due to two reasons: (I) the narrow thermal range in which this polymer can be melted and processed without significant thermal-induce detriment of molecular weight (most typically from 170 to 195 °C); (II) the complex rheology of the molten, which presents a sudden drop in viscosity at a certain temperature. Indeed, this rheological behavior can hinder the filament formation from the extruder head if the viscosity is too low, or limits the homogeneity of the compound in the heating chamber if the viscosity is too high. Adding a plasticizer can not only reduce the brittleness of this polymer at room temperature, but can also allow it to reach a suitable viscosity for the selected processing method at a lower temperature. With this purpose, PHB has been mixed with different quantities of GT (2.5, 5, and 10 wt%, detailed formulations in Table S1) using a twin-screw extrusion apparatus (details reported in the experimental section). The appropriate temperatures and screw rate suitable for Ex (see Table S2) have been determined experimentally, based on the melting temperature reported in the polymer datasheet. The temperature peak has been positioned in the central section of the heating chamber and gradually decreased towards the extrusion head, to facilitate the mixing process and prevent thermal degradation of the polymer. For this reason, a temperature profile has been selected with the lowest acceptable values for ensuring the processing, with a consistent material flow from the extrusion head exit.

The extruded materials have exhibited homogeneity (representative pictures in Figure S2) and continuous flow, although the noticed melt strength has not been sufficient to produce a windable filament [78]. The so-produced samples have been coded according to the wt% content of the added plasticizer as follows: PHB (neat polymer), PHB2.5GT, PHB5GT, and PHB10GT.

The thermal properties of the extruded compounds have been investigated using differential scanning calorimetry (DSC, details in the experimental section). The plasticizer intercalation among the polymeric chains induces a reduction of the interaction strength among the functional groups of the macromolecules. This also leads to an increased macromolecular mobility and reduced energy required to activate their movements [79]. This phenomenon is clearly visible in terms of glass transition temperature (T_g) reduction as shown in Fig. 2A (T_g values were extrapolated from the thermograms shown in Figure S4A). In particular, the neat PHB showed a T_g of 4 °C which decreased to 0 °C and −5 °C with only 2.5 and 5 wt% of GT respectively, indicating a significant plasticization effect. However, the addition of 10 wt% of GT did not result in further T_g reduction, which value is settled to approx. −4 °C similar to the PHB5GT.

DSC curves (Figure S4B) have been further processed to evaluate the effect of GT on the melting temperature (T_m), and crystallinity degree (X_c, calculated by Eq. (2) in the experimental section) of PHB. T_m represents an important parameter, for semicrystalline polymer as PHB, for evaluating the improvements in terms of processability in the molten state. As shown in Fig. 2B, by increasing the plasticizer content, the T_m has been reduced from 177 °C for the neat polymer to 175, 173, and 169 °C for 2.5, 5, and 10 wt% of GT, respectively. The reduction in the T_m has been also followed by a decrease in X_c (Fig. 2C). In particular, neat PHB exhibited X_c of 59 %, which decreased to 58 % for PHB2.5GT and to 52 % for PHB5GT, whereas 10 wt% of GT did not produce any further diminishing. Similarly, the plasticizing effect of GT was evident during the DSC analysis cooling scan. As shown in Figure S4C, the crystallization peaks of the formulations shifted to lower temperatures with increasing GT content, as reported in Table S4. Specifically, the crystallization temperature (T_c) of PHB decreased from 119 °C to 115 °C and 112 °C with the addition of 2.5 % and 5 wt% of GT, respectively. However, with 10 wt%, no further decrease in T_c was observed. After

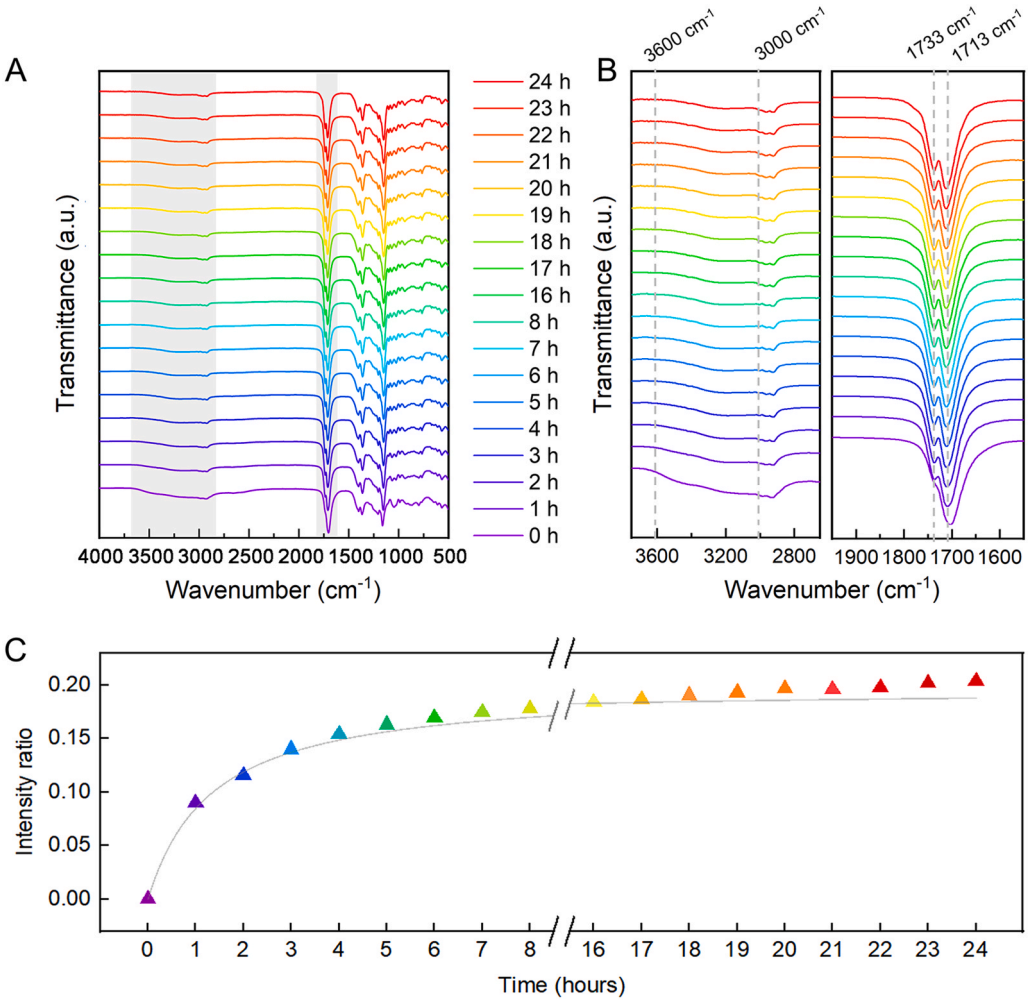

Fig. 1. (A) Full FT-IR spectra of the reaction mixture at different time points. The shaded areas represent the peaks highlighted in figure (B); (B) peaks used to follow the reaction progress. On the left the time decreasing peak of the hydroxyl groups (3600–3000 cm^{-1}) and on the right the arising peaks at 1733 cm^{-1} related to the ester bonds and the time-constant peak at 1713 cm^{-1} ascribable to the ketonic groups of LA. (C) Kinetics of the reaction obtained by FT-IR data analysis. Intensity ratio (calculated by Eq. 1) represents the ratio between the intensity of the peaks at 1733 cm^{-1} and 1713 cm^{-1}.

analyzing the experimental results, PHB5GT has been selected as the most promising formulation to compare GT with commercial plasticizers. PHB compounds have also been prepared with 5 wt% of ATBC and DINCH (composition reported in Table S1) using the same extrusion apparatus and processing parameters previously reported for GT compounds (Table S2). These two samples have been named PHB5ATBC and PHB5DINCH (representative pictures in Figure S2).

As shown in Fig. 2A, PHB5GT performed significantly better than both PHB5ATBC and PHB5DINCH in terms of T_g reduction, showing that the addition of the two commercial plasticizers causes only a negligible effect on the T_g when compared to the neat PHB. On the other hand, GT, ATBC, and DINCH plasticizers showed a similar effect on the decrease of T_m (Fig. 2B). GT outperformed the two commercial additives in reducing the crystalline fraction (Fig. 2C) and T_c (Figure S4C), which are mostly unaffected by the presence of ATBC and DINCH (DSC results are summarized in Table S4).

FT-IR analysis reported in Figure S3 has revealed no significant variations in terms of chemical structure between PHB and the different compounds. The spectra represent the plasticizers (peak assignment in Table S3) and the plasticized formulations. The unaltered structure indicates that the thermal processing has not resulted in detectable material degradation. Moreover, also the addition of plasticizers has not induced chemical modifications of the polymeric structure even after thermal processing.

The addition of plasticizers also typically affects the rheology of the polymer melt by reducing the intermolecular forces among polymer chains [80], which results in lowering the viscosity (thus increasing flowability) of the moulten. This clearly affects the melt processing conditions, such as temperature and shear rate, required to process the material. By studying the rheological behavior of polymer/plasticizer compounds, the processing conditions can be optimized, minimizing the time and energy required. The rheological properties of PHB/GT formulations have been tested at the representative temperature of 190 °C, in a shear rate range between 0.001 and 1000 s^{-1}. This shear rate range covers the typical values required for polymer processing techniques such as Ex, IM, and FDM [81,82]. All the samples displayed a shear-thinning behavior, with a decrease in viscosity as shear rate increased, due to the gradual alignment of the polymer chains [83]. As shown in Fig. 2D, the viscosity decreases by increasing the plasticizer content. Neat PHB has shown value of η_0 equal to 65 Pa•s, while it has been possible to achieve values of 53, 47 and 35 Pa•s with the formulation at 2.5, 5, and 10 wt% of GT, respectively. Over the entire studied range of shear rates, the highest concentration of GT (10 wt%) led to a substantial decrease in viscosity compared to lower contents of the plasticizer (2.5 and 5 wt%), as expected. Although the rheological properties of PHB2.5GT and PHB5GT were almost identical from 0.001 to 1 s^{-1}, the two compounds started diverging after shear rate values of 1 s^{-1}, with the PHB5GT that exhibits a more pronounced viscosity

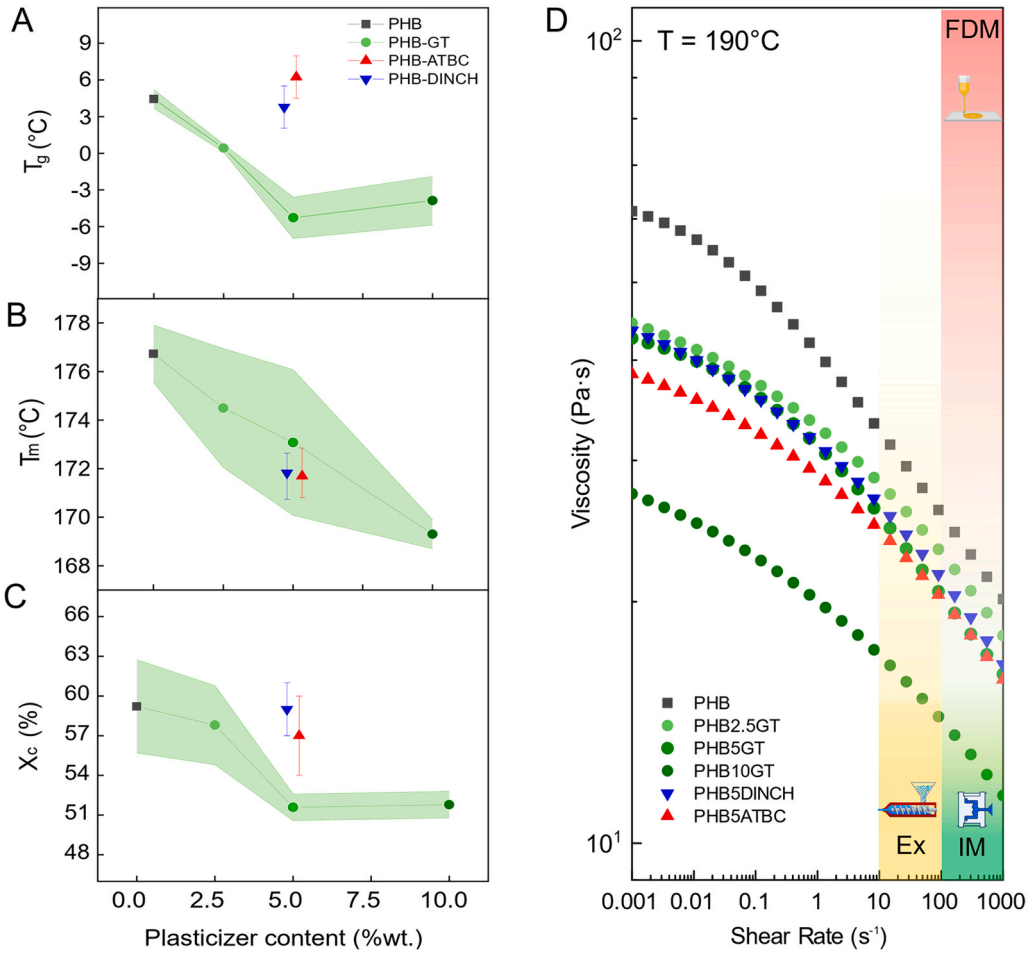

Fig. 2. (A) Glass transition temperature (T_g), (B) melting temperature (T_m) and (C) crystallinity degree (X_c, calculated by Eq. 2) of neat PHB, PHB/GT compounds and PHB compounded with 5 wt% of ATBC and DINCH. (D) Rheological behavior at 190 °C of neat PHB and its compounds with GT, ATBC and DINCH. The shaded areas represent the typical range of shear rate for extrusion (Ex, yellow), injection-molding (IM, green) and fused deposition modelling (FDM, red).

reduction. The differences between PHB2.5GT and PHB5GT become more and more significant from 10 to 100 s^{-1}, which is the typical shear rate range at which Ex operates [81]. Similarly, the decrease in viscosity is even more noticeable in the range from 100 to 1000 s^{-1}, which is typical for IM [81] and FDM [82]. Additionally, the rheological properties of PHB5ATBC and PHB5DINCH have been investigated using the same analysis conditions, to compare the plasticization effects. As reported in Fig. 2D, PHB5ATBC shows a η_0 of 46 Pa•s, performing comparably to PHB5GT. On the contrary, PHB5DINCH presentes a η_0 of 54 Pa•s, similar to what is obtained with PHB2.5GT. In the shear rate regime at which Ex, IM, and FDM operate, the commercial formulations (with ATBC and DINCH) presente viscosity values comparable to the one obtained with 5 wt% GT, overall. Based on the rheological results, GT appears to be a promising bio-based alternative plasticizer for PHB.

The addition of a plasticizer can also importantly influence the mechanical properties of a polymer [41]. To analyze the mechanical behavior of the plasticized PHB formulations, dog-bone specimens have been produced through injection molding (Figure S5). The main parameters such as temperature, shot size, cooling time, and extraction time (reported in Table S5) have been optimized during the process. To ensure the material a proper fluidity for the injection, the temperature in the plasticization cylinder has been kept constant at 180 °C, just slightly above the T_m of neat PHB. It is important to underline that, compared to neat PHB, the temperatures of the injection cylinder and nozzle has been decreased by 5 °C (170 °C) for PHB2.5GT, PHB5GT, PHB5ATBC and by 10 °C for PHB10GT. On the other hand, for PHB5DINCH, the temperatures remained unchanged (180 °C) as for pristine PHB. The possibility of a decrease in the injection temperature is a clear sign of the increased fluidity of the material due to the plasticizer, in accordance with the rheological tests (Fig. 2D). The so obtained specimens did not show any significant difference, except for slight chromatic variations due to the color of the plasticizer (Figure S5). The reduction in the injection temperatures did not affect the final appearance of the samples, but it certainly limited the effects of thermal degradation.

The specimens have been used in Dynamic Mechanical Analysis (DMA) tests to better understand the viscoelastic behavior of the polymeric compounds. The DMA results have been divided and analyzed into two distinct data sets. The first set (referred to as the *GT series*) consists of neat PHB and PHB/GT compounds, to investigate how the different content of additive affects the properties of pristine PHB (Fig. 3A). The second set (referred to as the *5 % series*) of data allows to compare the properties of neat PHB and PHB plasticized with 5 wt% of GT, ATBC and DINCH (Fig. 3B).

Within the *GT series*, as expected, the increase in plasticizer content caused a storage modulus (*E'*) reduction over the entire temperature range analyzed. According to Scandola *et al.*, this reduction can be attributed to the crystalline content of the polymer, which decreases with the increasing amount of plasticizer [84], as indeed observed in this case (Fig. 3A).

The loss modulus (*E''*) is related to the rheological behavior of the material and represents the energy dissipated in the irreversible movement of the polymer chains. In Fig. 3A, it is possible to notice a shift in the *E''* curves towards lower temperatures, as well as an increase in the subtended area, as the amount of GT in the polymer increases. This

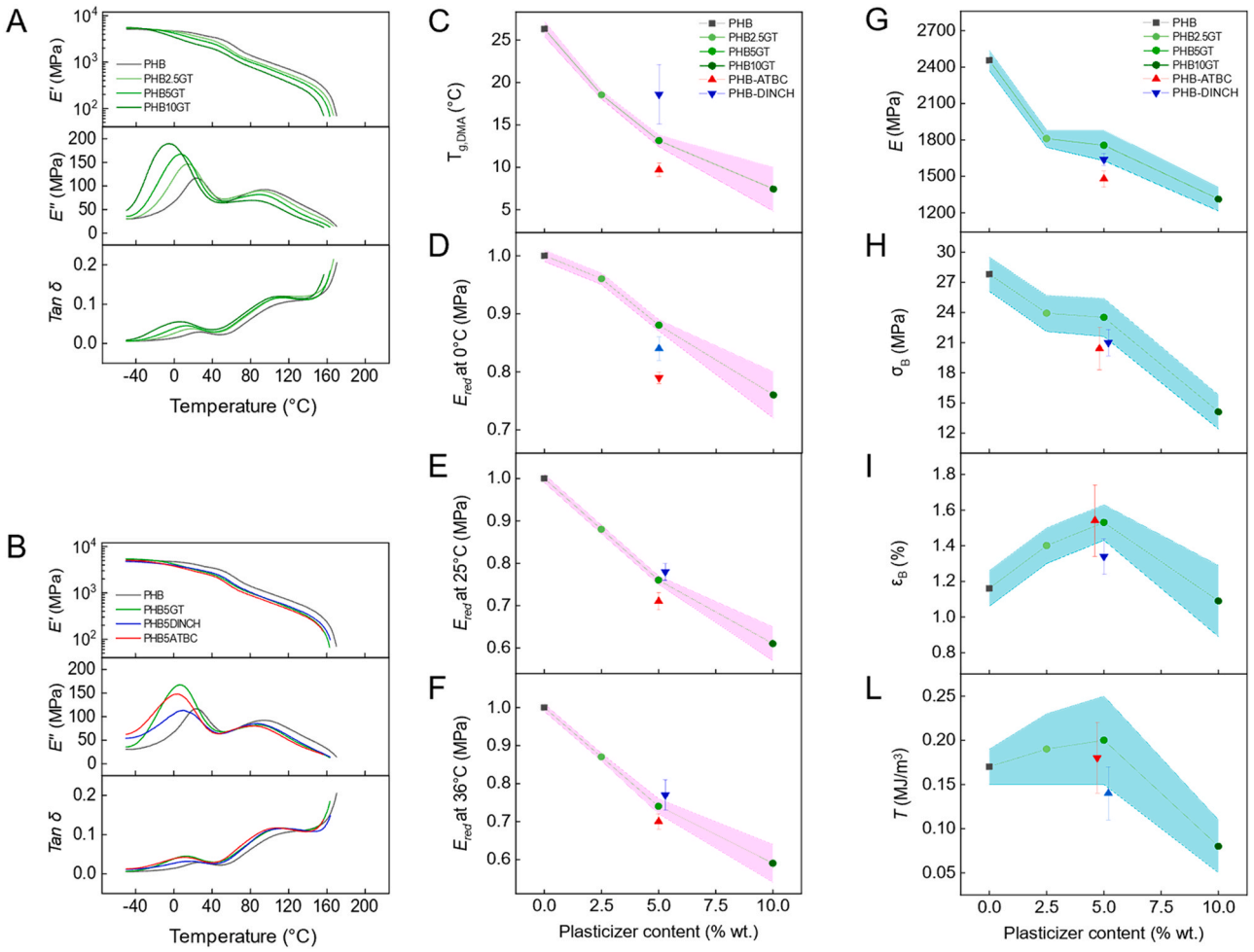

Fig. 3. Storage modulus (*E'*), loss modulus (*E''*) and loss factor (Tanδ), from DMA tests, of (A) neat PHB and PHB/GT compounds and (B) neat PHB and 5 wt% of GT, DINCH and ATBC. (C) Glass transition temperature from DMA data ($T_{g,DMA}$); E_{red} (calculated by Eq. (3)) extrapolated at (D) 0 °C, (E) 25 °C and (F) 36 °C, as a function of the GT content. (G) elastic modulus *(E)*, (H) tensile strength (σ_B), (I) elongation at break (ε_B) and (L) toughness (*T*) as a function of the GT content, obtained by UTT.

suggests that an increasingly larger fraction of the energy is used for chain relaxation at a lower temperature, indicating an effective plasticization.

The damping factor (Tanδ) curves, obtained by the ratio between *E''* and *E'* (Fig. 3A), show by the first peak corresponding to the glass transition temperature ($T_{g,DMA}$), which can be attributed to β relaxation [84]. The addition of GT caused the peak to broaden and shift, indicating the early onset of the transition and shift of $T_{g,DMA}$ to lower values. In fact, the reduction in $T_{g,DMA}$ is the main effect obtained and exploited by the addition of a plasticizer to a rigid polymer, resulting in improved flexibility [36]. The second peak observed in the Tanδ curves, between the glass transition and melting, can be associated with the α relaxation, related to the mobility of more extended segments of the polymeric chains [85]. Again, the start of the transition is shifted to lower temperatures, proportionally to the plasticizer content. Both effects on *E'* and Tanδ can be attributed to the uniformly distributed plasticizer molecules, that can weaken the intermolecular interactions among polymer chains, thus increasing the free volume [41,70].

The Fig. 3B reports the DMA curves of the *5 % series*. The *E'* values of the plasticized formulations with 5 wt% of GT, DINCH, and ATBC are lower compared to the neat PHB. It is noteworthy that PHB5GT has shown a reduction of *E'* modulus that is comparable to that obtained with ATBC, considered the most effective citrate-based plasticizers for PHAs [86]. As reported in Fig. 3C and in Table S6, all the plasticized formulations have shown a decrease in $T_{g,DMA}$ if compared to neat PHB.

To further highlight the effect of the plasticizer on the thermo-mechanical behavior of the PHB, the reduced modulus (E_{red}), expressed as the ratio between the storage modulus of a compound (E'_{i-th}) and the pristine polymer (E'_{PHB}) is shown in Fig. 3. E_{red} was calculated using Eq. 3 (details in the experimental section) at different temperatures: at 0 °C (below the T_g, Fig. 3D), at 25 °C (room temperature, Fig. 3E), and at 36 °C (mean body temperature, Fig. 3F), considering the potential applications of PHB in the biomedical field [87].

The E_{red} decreases with the increase of the GT content for all analyzed temperatures (Fig. 3D–F). It is also possible to observe that E_{red} decreases more significantly for temperatures above the glass transition ($T_{g,DMA}$ and E_{red} are listed in Table S6), indicating an increased plasticization efficiency in the conditions where materials is most likely to be used or processed. For example, for PHB5GT, below T_g the E_{red} is reduced by about 12 %, while above T_g the reduction reaches a value of over 24 %, compared to the reference value of neat PHB. A similar trend can be also observed when a different content of plasticizer is used.

The comparison of E_{red} between GT and the commercial plasticizers reveals similar behavior, especially for 25 and 36 °C (Fig. 3D–F).

The hindering effect on the intermolecular forces among macromolecular chains, due to intercalated plasticizer molecules, can cause not only a decrease in T_g but also an increase in flexibility and strain at break. For this reason, the mechanical behavior of PHB and plasticized formulations have been further explored through Uniaxial Tensile Test (UTT). In particular, Young's modulus (*E*), tensile strength (σ_B),

elongation at break (ε_B), and toughness have been investigated to evaluate the effect of the plasticizer on mechanical properties (all data are collected in Table S7). PHB is known as a polymeric material characterized by a high stiffness and limited elongation at break [88], the compounding with GT caused a significant reduction in the E and a slight decrease in σ_B, compared to pristine PHB. Specifically, 2.5 and 5 wt% GT produced a decrement in stiffness of 26 and 28 % (Fig. 3G), and a reduction in σ_B of 14 and 16 % (Fig. 3H), respectively. Considering the typical high brittleness of PHB and the relatively low additive content used (2.5 and 5 wt% GT), the obtained increase in ε_B of 21 and 32 % (Fig. 3I) must be considered a remarkable result to narrow the mechanical gap between conventional plastic commodities and PHB. Regarding the sample PHB10GT, E decreased following the trend of the other formulations, whereas σ_B has shown a considerable drop of −49 % (Fig. 3G and H). The ε_B did not constantly grow with the GT content, decreasing by 6 % with comparison to pristine PHB (Fig. 3I) when 10 wt % GT is compounded with the polymer. Interestingly, from these mechanical tests, 5 wt% represents the best compromise between reduced stiffness and increased elongation at break. Moreover, the herein proposed plasticizer, when added at 5 wt%, had an effect on the mechanical properties comparable to different commercial plasticizers (ATBC and DINCH) added at the same concentration (Fig. 3G–I). As a consequence, the incorporation of GT also results in an enhancement in toughness *(T)* compared to neat PHB. Once again PHB5GT was found to be the best overall formulation considering that T drops when the additive content is further increased to 10 wt% (Fig. 3L). Furthermore, PHB5GT and PHB5ATBC present a similar T increment of (0.20 and 0.18 MJ•m^{-3}, respectively), compared to neat PHB (0.17 MJ•m^{-3}). On the other hand, a decrease to 0.14 MJ•m^{-3} for PHB5DINCH has been found, confirming the trend already observed with the other mechanical parameters, previously described.

The UTT results further confirm that the hindrance of GT molecules can effectively increases the free space among macromolecular chains, thus limiting the intermolecular forces and increasing their mobility.

The compounds produced via twin screw extrusion were then processed using a single screw extruder (parameters detailed in Table S8) to create a filament suitable for the 3D printing of porous scaffolds. These scaffolds have potential biomedical applications [89,90] such as bone tissue regeneration, thanks to the previously demonstrated non-toxicity of GT [69]. These customizable constructs are designed to mimic the complex structure of natural bones and provide a suitable support for cell ingrowth and vascularization. In fact, scaffolds for bone regeneration are usually designed with open and interconnected porous architecture that allows the diffusion of nutrients into the scaffold and the removal of metabolic wastes resulting from cellular activity [91]. Cylindrical scaffolds (Fig. 4A) have been 3D printed, by FDM technique, using different temperatures and plasticizer concentrations to optimize the print quality of the scaffolds.

A temperature of 200 °C has been initially selected for all formulations and gradually reducing by 5 °C at each step until reaching 180 °C. In accordance with the T_m observed by DSC analysis (Fig. 2B), a further reduction of the printing temperature below 180 °C did not lead to a complete melting and an appropriate viscosity of the molten polymer.

The printed porous scaffolds have been analyzed through optical microscopy to investigate the quality of the printed object, as a function of both the printing temperature and compound composition. As a general remark, the use of GT results in the reduction of the printing temperature up to 20 °C, while maintaining the same resolution obtained with pure PHB filament printed at 200 °C (Fig. 4A). This is a very significant result since it is well-known that 200 °C is the onset temperature where the thermal degradation process leads to a quick and uncontrollable drop of PHB molecular weight [92,93]. With 2.5 wt% of GT, good printing quality has been achieved by employing a temperature of 190 °C. A further decrease of 10 °C (printing temperature = 180 °C, Fig. 4A) has been achieved for both PHB5GT and PHB10GT samples. It is noteworthy that for the PHB5GT scaffold (Fig. 4A) the printing resolution is completely comparable to the neat PHB scaffold printed at 200 °C. On the contrary, in the PHB10GT sample (Fig. 4A) the filament begins to thin out losing some regularity in the unsupported areas, leading to a drop-like shape in the strand where the extruded filament is deposited at the intersection points of the raster. This behavior might be associated to the significant decrease in the viscosity of the molten

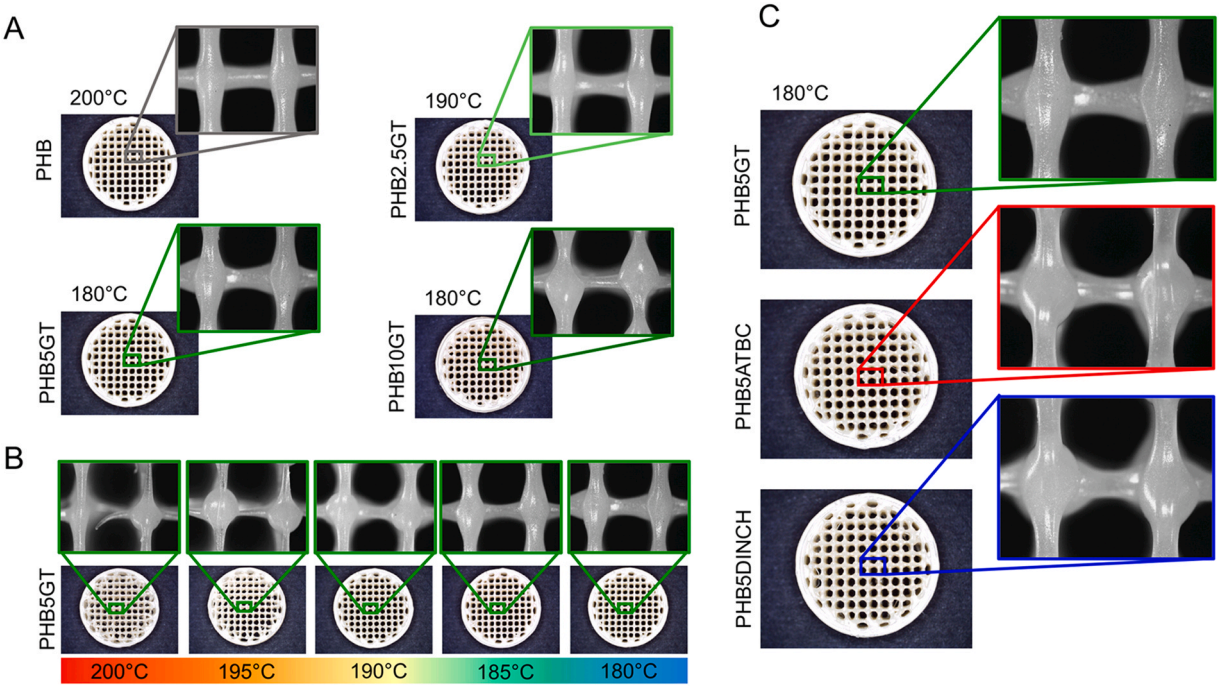

Fig. 4. Optical images of the 3D-printed scaffolds at different temperatures and GT concentration. A) Scaffolds printability increasing GT concentration; B) scaffolds, obtained with PHB5GT formulation, printed at increasing temperatures from 180 to 200 °C; C) scaffolds printed at 180 °C with three different plasticizers (5 wt%), respectively GT, ATBC and DINCH. In the insets the internal strands of the scaffolds are shown in detail.

compound, as shown in Fig. 2D.

Therefore, the PHB5GT formulation has been selected as a benchmark for further investigations. In particular, by increasing the printing temperatures from 180 to 200 °C, the filament became less and less viscous and tended to thin out, especially in the unsupported sections of the print. At the highest tested temperatures (195 and 200 °C) the thinning became very significant and led to the break of the strand, interrupting the continuity of the filling geometry, as shown by Fig. 4B. The most regular and continuous deposition of the filament has been obtained at 180 °C (Fig. 4B). Moreover, at this temperature, the internal pores of the scaffold have maintained a squared geometry over the entire surface area and even near the external border, with a resolution very similar to the one obtained for neat PHB printed at 200 °C. The printability of PHB5GT at 180 °C, has also been compared to the corresponding formulations with commercial ATBC and DINCH. Fig. 4C shows that 5 wt% of the two commercial plasticizers leads to small irregularities where the filaments of two consecutive layers overlap and therefore to a loss in printing resolution when compared to PHB5GT.

Based on the UTT, DSC and DMA investigations, the herein presented PHB compounds exhibits a suitable stiffness over a wide temperature range, high crystallinity and T_m, making these materials a potential solution for repairing bone and cartilage defects [15]. In this context, the possibility to fabricate scaffolds through FDM 3D printing with precise shape and porosity control, facilitated by the enhanced processability achieved through the incorporation of bioplasticizers, makes these materials highly attractive for a wide range of biomedical prototypes [94].

3. Conclusions

The growing interest in the use of PHB in various applications has driven research toward additives that allow this promising biopolymer to become a valuable alternative to the fossil-based commodity plastics. To achieve this, the limited melt processability and mechanical properties of PHB must be improved and, at the same time, the biodegradability and biocompatibility typical of the PHAs polymer family must be preserved.

In this work, PHB has been compounded with GT bioplasticizer and the plasticization effect has been compared with two commercial plasticizers (ATBC and DINCH) that have recently raised several health concerns. The synthesis of GT has been optimized by kinetics study, obtaining an increase in molar yield of the reaction up to 82 % and a reduction in the reaction time to 16 h.

GT allowed to achieve an effective plasticization, as expressed by the reduction of the glass transition temperature of PHB evaluated by both DSC and DMA. DSC also revealed a decrease in both the melting temperature and the crystallinity degree by increasing GT content. These parameters also have an important effect on the mechanical properties of PHB. In particular, with only 5 wt% of GT, the flexibility has been increased (elastic modulus reduced up to 28 %) with an overall increase in toughness of approximatively 10 %. Furthermore, the rheological analysis highlighted a shear thinning behavior with a decrement in the melt viscosity as a function of the plasticizer content. Based on these results, 5 wt% of GT appears to be the best compromise to have an effective plasticization of PHB and minimize the leaching, which is known to increase with the additive content.

The plasticization effect of GT on PHB has been also compared with that of the compounds containing ATBC and DINCH commercial plasticizers. Overall, GT can enhance mechanical, thermal, and rheological properties to a degree that matches or even exceeds the performance of the commercial plasticizers, establishing it as a viable and sustainable green alternative. Moreover, an enhanced melt processability was observed, allowing to reduce the AM processing temperature from 200 to 180 °C, thus significantly expanding the PHB's processability thermal range. This temperature and viscosity reduction is also promising for facilitating the printing suitability. In particular, 3D printing through FDM technique allowed to successfully obtain scaffolds potentially suitable for bone and tissue regeneration, at 20 °C lower than the most typical printing temperature. In comparison to ATBC and DINCH, the use of GT leads to smoother and more homogeneous scaffolds, with deposition of more uniform strands and minimizes the strand distortions at the junctions between two layers.

The herein presented results confirm that GT can represent a valuable and safer alternative to the currently available commercial "green" plasticizer for biopolyesters. In particular, using GT it is possible to overcome well-known disadvantages that limit the diffusion of PHB as replacement of the plastic commodities.

4. Experimental

4.1. Materials

The following listed reagents were all supplied by Sigma-Aldrich and used for the synthesis of the glycerol trilevulinate (GT) plasticizer: levulinic acid (LA, 98.0 %), glycerol (GLY, ≥ 99 %), water (HPLC grade), sodium sulfate (Na_2SO_4, anhydrous, ≥ 99 %), and sodium chloride (NaCl). Additionally, sodium bicarbonate ($NaHCO_3$, ≥ 99.5 %, obtained from Carlo Erba), p-toluenesulfonic acid monohydrate (PTSA, 98.5 %, obtained from Alfa Aesar), ethyl acetate (EtAc, 99.96 %, obtained from Fischer Chemicals) and deuterated chloroform ($CDCl_3$, 99.8 atom% D, contains 0.03 % v/v tetramethylsilane TMS, supplied by WVR Chemicals) were used. All above-mentioned reagents and solvents were used as-received without further purification.

Polyhydroxybutyrate (PHB) was obtained from Gruppo MAIP (Iam-NATURE B6 T P001Y, M_w 240,000 g mol^{-1}). The polymer was analyzed by nuclear magnetic resonance (^{1}H NMR) to obtain detailed information on its composition. The related experimental procedure is reported in the supporting information followed by ^{1}H NMR spectrum in Figure S7. The ^{1}H NMR investigation showed the presence of 0.3 % mol (calculated by Equation S1 in supporting information) of 3-hydroxyvaleric acid units (3HV) with respect to 3-hydroxybutyric acid (3HB). This negligible amount of 3HV units cannot produce significant modification of the polymer properties. The commercial plasticizers 1,2-cyclohexane dicarboxylic acid diisononyl ester (Hexamoll® DINCH) and acetyl tributyl citrate (ATBC, ≥ 98 %) were obtained from BASF and Sigma Aldrich, respectively.

4.2. Plasticizer synthesis

The GT solvent-free synthesis and product purification were carried out adjusting the procedures reported elsewhere [69]. In brief, GLY 4.758 g/0.0517 mol, LA 30 g/0.2585 mol and PTSA catalyst 0.445 g/0.00259 mol (5 % mol. with respect to GLY) were placed in a round-bottom flask and heated up to 110 °C for 24 h (in an oil bath) under magnetic stirring, leaving the flask open. Afterwards, the mixture was cooled down at room temperature and quenched with a saturated $NaHCO_3$ (aq) solution to neutralize the excess of LA. The solution was then extracted twice, by a separation funnel, with EtAc. The extracted organic phase was washed two further times with saturated $NaHCO_3$ (aq) and once with saturated NaCl (aq) solution. After drying over anhydrous Na_2SO_4, the residual solvent was evaporated with a rotary evaporator under reduced pressure until a yellowish viscous product was obtained. The reaction yield and selectivity were optimized studying the reaction kinetics, mainly varying reaction time.

4.3. Fourier Transform Infra-Red Spectroscopy

The reaction was monitored through Fourier Transform Infra-Red Spectroscopy (FT-IR). Spectral data were obtained using a Perkin Elmer Spectrum Two spectrometer that featured a diamond attenuated total reflection crystal (ATR). Each spectrum was collected by recording 16 scans and the selected spectra window ranged from 4000 to 400 cm^{-1}. The data obtained from the spectra were processed using

Spectrum 10 software (PerkinElmer). The progress of the reaction was monitored by calculating the ratio between the intensity of the peaks at 1713 and 1733 cm^{-1} with Eq. (1):

$$Intesity\ ratio = [T_{1713cm^{-1}}(\%) - T_{1733cm^{-1}}(\%)]/T_{1733cm^{-1}}(\%) \quad (1)$$

Intensity ratio was plotted *vs.* reaction time and the data were fitted by the modified Hill function with offset (by Origin Pro, version 9.8.200).

The same FT-IR setup was used to conduct the structural analysis on the polymer, pure plasticizer and compounds.

4.4. Nuclear Magnetic Resonance

To confirm the chemical structure of GT and to evaluate the composition of the PHB, 1D Nuclear Magnetic Resonance (NMR) spectroscopy was employed. ^{1}H NMR spectra were recorded at room temperature using a Varian Mercury 400 instrument running at 400 MHz (nominal frequency: 399.96 MHz). The solvent used was $CDCl_3$ containing 0.03 % vol. of tetramethylsilane (TMS) as the internal reference. Chemical shifts (δ) were reported in parts per million (ppm) relative to the residual solvent signals ($CHCl_3$ at 7.26 ppm). The NMR spectra were processed using MestReNova software (Mestrelab Research S.L.).

4.5. Compounds preparation

The PHB granules, with original dimensions of 2–4 mm, were ground using an analytical mill (IKA A11 basic) in cryogenic conditions. Liquid nitrogen (N_2) was used during this phase to lower the temperature below the glass transition temperature (T_g), increasing the brittleness and allowing better grinding, obtaining granules with dimensions lower than 2 mm. This step was necessary to be able to subsequently process the polymer with the twin screw extruder. Ground polymer and plasticizer were pre-mixed in the analytical mill under room conditions according to the compositions listed in Table S1. Before extrusion, the premixes were dried at 40 °C for 4 h in the oven, to remove any residual moisture that could cause inhomogeneity during the extrusion process. The pre-mixed materials were processed using a co-rotating twin screw extruder (RES-2 P/12A Explorer Extruder, Zamac Mercator, Poland), having an 11 mm screw diameter and a 40 L/D screw ratio. The equipped screws have a variable profile along their length, which allowed the homogenization of the melt by compacting and transporting the polymer from the hopper zone to the extrusion head. The temperature profile in the six heating zones of the screws is shown in Table S2 and it was kept the same for all the treated compositions. The maximum temperature was set in zones 3 and 4, corresponding to the mixing section of the screws, to lower the viscosity of the polymer and homogenize it with the plasticizer. The temperature was then lowered again toward the head (zones 5 and 6) to achieve a consistency more suitable for extrusion. The extruded blends were collected, air-cooled, and reduced to pellets (Figure S2) using a shredder (Felfil, Italy). The pellets obtained were used to produce injection-molded dumbbell specimens and 3D printing filaments. The pellets obtained after the twin screw processing were partially used to produce injection-molded specimens through a Babyplast 10/12, equipped with a mold of a model 5 A dumbbell-shaped specimen according to ISO 527 standard. The parameters used for the injection molding are reported in Table S5.

4.6. Single screw filament extrusion

The other part of the pellet obtained after twin screw processing was used to get filament suitable for 3D printing. For this purpose, a benchtop extrusion system (Felfil Srl., Italy), composed of a single screw extruder equipped with a cooling fan array was used. The diameter of the filament (Figure S2) was set to 1.55 ± 0.1 mm by an optical control equipped with the spooler. Extrusion parameters are reported in Table S8.

4.7. 3D printing

3D printed scaffolds were designed with SolidWorks software, having a cylindrical geometry of 15 mm in diameter and 5 mm in height. The objects were obtained using a Prusa i3 MK3S+ printer equipped with a 0.4 mm nozzle, setting the printing parameters in the PrusaSlicer software. Specifically, layer height was set at 0.2 mm and strand width was set at 0.4 mm, infill density, and geometry were set to 30 % and linear, respectively, alternating the infill direction by 90° between adjacent layers, printing speed was set to 25 mm•min^{-1}, and finally extrusion flow was set to 1.1. The cylinders were printed with 2 wall loops and 0 top/bottom layers. All scaffolds were printed with a 4 mm brim support and some glue to ensure adequate adhesion to the printing plate, which was heated at a temperature of 60 °C. The printing temperature range between 200 and 180 °C was investigated.

4.8. Material characterizations

Differential Scanning Calorimetry (DSC) was used to measure the thermal properties, such as the melting temperature (T_m), glass transition temperature (T_g), crystallinity degree (X_c) and crystallization temperature (T_c) of both neat and plasticized polymeric samples. The DSC analysis was performed using a Q10 instrument from TA Instruments . The DSC cell was equipped with a Discovery Refrigerated Cooling System (RCS90) and operated under a nitrogen atmosphere with a purge flow rate of 20 mL min^{-1}. Approximately 10 mg of each sample were initially cooled down to −60 °C. The samples were then heated up to 200 °C at a heating rate of 20 °C min^{-1}. After a cooling step at a rate of 10 °C min^{-1} to −60 °C, the samples were heated for a second time at a rate of 10 °C min^{-1} up to 200 °C. The crystallinity degree (X_c) of the samples was calculated using Eq. (2):

$$Xc(\%) = \Delta H_m / \Delta H_m^0 \bullet 100 \quad (2)$$

which takes into account the melting enthalpy (ΔH_m) obtained from the DSC measurement and the melting enthalpy of the 100 % crystalline polymer (ΔH_m^0). For the calculation, the selected enthalpy of melting for 100 % crystalline PHB was determined to be 146 J•g^{-1} [95,96]. Three samples were measured for each formulation to ensure repeatability.

DSC curves were processed with TA Universal Analysis 2000 software (TA Instruments) to extrapolate the T_m and ΔH_m from the first heating scan, T_c from the cooling scan and T_g from the second heating scan.

Viscosity measurements under steady-state conditions were conducted using a rotational rheometer Physica MCR 301 (Anton Paar, GmbH Austria), which was equipped with a Peltier heating system and a solvent trap kit. The shear-rate viscosity correlation was analyzed at a temperature of 190 °C, with the range of shear rates varying between 0.01 and 100 s^{-1}. For these experiments, a cone-plate geometry (CP50–1) with a diameter of 50 mm, an angle of 0.989°, and a gap of 99 μm was used. The experimental data obtained from steady-state viscosity measurements were fitted with the Carreau-Yasuda model [97] to calculate the zero-shear viscosity η_0. All experiments were performed three times to ensure the results repeatability.

Dynamic Mechanical Analysis (DMA) was conducted in duplicate on the prepared samples using a TA Q800 instrument. The test was performed following the ASTM D7028 standard with a single cantilever clamp in a temperature ramp mode, applying the following parameters: 10 μm for the amplitude strain deformation, 1 Hz frequency, temperature range from −60 to 175 °C, with initial isothermal soak time of 10 min, and temperature ramp 3 °C•min^{-1}. Before testing, the samples were stored under vacuum at room temperature. The values of storage modulus (E'), loss modulus (E''), and damping factor (Tanδ) were collected and reported as a function of the temperature. The glass transition temperature ($T_{g,DMA}$) was obtained from the maximum of the Tanδ curve. Based on E' values obtained from the DMA analysis, the

reduced modulus (E_{red}) was calculated according to Eq. (3) [98]:

$$E_{red} = E'_{i-th}/E'_{PHB} \quad (3)$$

Mechanical properties were tested by performing the uniaxial tensile test (UTT) on the injection molded specimens. Measurements were conducted with a 112 TesT GMBH Universal Testing Machine (Germany), with a 2 kN load cell. Ten specimens of pure PHB and each plasticized material were tested at a constant tensile speed of 0.5 mm•min^{-1}, at room temperature (approx. 25 °C). The test was considered completed at specimen failure. Tensile properties such as Young's modulus (E), tensile strength (σ_B), elongation at break (ε_B), and toughness (T) were recorded and compared [99].

The optical Optika B-380 series (Optika Srl, Italy) microscope was used to observe the macroscopical appearance of the printed scaffolds and evaluate the quality of the individual deposited strands.

Funding

Davide Morselli and Paola Fabbri received financial support by the European Union–NextGenerationEU (National Sustainable Mobility Center CN00000023, Italian Ministry of University and Research Decree no. 1033-17/06/2022, Spoke 11–Innovative Materials & Lightweighting). The opinions expressed are those of the authors only and should not be considered as representative of the European Union or the European Commission's official position. Neither the European Union nor the European Commission can be held responsible for them.

Daniel Milanese received financial support from the ECOSISTER project funded under the National Recovery and Resilience Plan (NRRP), Mission 04 Component 2 Investment 1.5 - NextGenerationEU, Call for tender n. 3277 dated 30/12/2021, Award Number: 0001052 dated 23/06/2022.

CRediT authorship contribution statement

Davide Morselli: Writing – review & editing, Writing – original draft, Visualization, Supervision, Resources, Data curation, Conceptualization. **Corrado Sciancalepore:** Writing – review & editing, Writing – original draft, Supervision, Resources, Data curation, Conceptualization. **Daniel Milanese:** Funding acquisition. **Paola Fabbri:** Funding acquisition. **Maila Castellano:** Writing – original draft, Supervision, Investigation, Data curation. **Micaela Degli Esposti:** Writing – original draft, Visualization, Supervision, Resources. **Luca Lenzi:** Writing – review & editing, Writing – original draft, Visualization, Investigation, Data curation. **Elena Togliatti:** Writing – review & editing, Writing – original draft, Visualization, Investigation, Data curation.

Declaration of Competing Interest

The authors declare that they have no known competing financial interests or personal relationships that could have appeared to influence the work reported in this paper.

Data availability

Data will be made available on request.

Acknowledgments

The authors acknowledge Mr Haseeb Ali for the technical support in the synthesis and purification of the bioplastyicizer.

Appendix A. Supporting information

Supplementary data associated with this article can be found in the online version at doi:10.1016/j.addma.2024.104290.

References

[1] P. Stegmann, M. Londo, M. Junginger, The circular bioeconomy: its elements and role in European bioeconomy clusters, Resour. Conserv. Recycl.: X 6 (2020) 100029, https://doi.org/10.1016/j.rcrx.2019.100029.
[2] M. Lettner, J.P. Schöggl, T. Stern, Factors influencing the market diffusion of bio-based plastics: results of four comparative scenario analyses, J. Clean. Prod. 157 (2017) 289–298, https://doi.org/10.1016/J.JCLEPRO.2017.04.077.
[3] P.F.H. Harmsen, M.M. Hackmann, H.L. Bos, Green building blocks for bio-based plastics, Biofuels Bioprod. Bioref. 8 (2014) 306–324, https://doi.org/10.1002/BBB.1468.
[4] J.C. Philp, R.J. Ritchie, J.E.M. Allan, Biobased chemicals: the convergence of green chemistry with industrial biotechnology, Trends Biotechnol. 31 (2013) 219–222, https://doi.org/10.1016/j.tibtech.2012.12.007.
[5] A.Z. Naser, I. Deiab, B.M. Darras, Poly(lactic acid) (PLA) and polyhydroxyalkanoates (PHAs), green alternatives to petroleum-based plastics: a review, RSC Adv. 11 (2021) 17151–17196, https://doi.org/10.1039/D1RA02390J.
[6] A. Costa, T. Encarnação, R. Tavares, T. Todo Bom, A. Mateus, Bioplastics: innovation for green transition, Polymers 15 (2023) 517, https://doi.org/10.3390/POLYM15030517.
[7] J.G. Rosenboom, R. Langer, G. Traverso, Bioplastics for a circular economy, Nat. Rev. Mater. (2022) 117–137, https://doi.org/10.1038/s41578-021-00407-8.
[8] S. Guleria, H. Singh, V. Sharma, N. Bhardwaj, S.K. Arya, S. Puri, M. Khatri, Polyhydroxyalkanoates production from domestic waste feedstock: a sustainable approach towards bio-economy, J. Clean. Prod. 340 (2022) 130661, https://doi.org/10.1016/J.JCLEPRO.2022.130661.
[9] C.O. Tuck, E. Pérez, I.T. Horváth, R.A. Sheldon, M. Poliakoff, Valorization of biomass: deriving more value from waste, Science 337 (1979) (2012) 695–699, https://doi.org/10.1126/SCIENCE.1218930.
[10] J. Zhang, E.I. Shishatskaya, T.G. Volova, L.F. da Silva, G.Q. Chen, Polyhydroxyalkanoates (PHA) for therapeutic applications, Mater. Sci. Eng.: C 86 (2018) 144–150, https://doi.org/10.1016/J.MSEC.2017.12.035.
[11] Y. Doi, K. Mukai, K. Kasuya, K. Yamada, Biodegradation of biosynthetic and chemosynthetic polyhydroxyalkanoates, Stud. Polym. Sci. 12 (1994) 39–51, https://doi.org/10.1016/B978-0-444-81708-2.50010-5.
[12] M. Saavedra del Oso, M. Mauricio-Iglesias, A. Hospido, B. Steubing, Prospective LCA to provide environmental guidance for developing waste-to-PHA biorefineries, J. Clean. Prod. 383 (2023) 135331, https://doi.org/10.1016/J.JCLEPRO.2022.135331.
[13] Z. Li, J. Yang, X.J. Loh, Polyhydroxyalkanoates: opening doors for a sustainable future, NPG Asia Mater. 2016 8 (4) (2016), https://doi.org/10.1038/am.2016.48 e265–e265.
[14] J.K. Muiruri, J.C.C. Yeo, X.J. Loh, G.Q. Chen, C. He, Z. Li, Poly(hydroxyalkanoates) (PHAs) based circular materials for a sustainable future, Circ. Plast.: Sustain., Emerg. Mater., Valoriz. Waste Plast. (2023) 273–303, https://doi.org/10.1016/B978-0-323-91198-6.00002-4.
[15] M. Ferri, E.M.S. Chiromito, A.J.F. de Carvalho, D. Morselli, M. Degli Esposti, P. Fabbri, D. Morselli, C. De Maria, Fine tuning of the mechanical properties of bio-based PHB/nanofibrillated cellulose biocomposites to prevent implant failure due to the bone/implant stress shielding effect, Polymers (Basel) 15 (2023), https://doi.org/10.3390/polym15061438.
[16] A. Lapomarda, M. Degli Esposti, S. Micalizzi, P. Fabbri, A.M. Raspolli Galletti, Valorization of a levulinic acid platform through electrospinning of polyhydroxyalkanoate-based fibrous membranes for in vitro modeling of biological barriers, ACS Appl. Polym. Mater. 4 (2022) 5872–5881, https://doi.org/10.1021/acsapm.2c00721.
[17] A. Genovesi, C. Aversa, M. Barletta, Polyhydroxyalkanoates-based cast film as bio-based packaging for fresh fruit and vegetables: manufacturing and characterization, J. Polym. Environ. 31 (2023) 4522–4532, https://doi.org/10.1007/S10924-023-02914-X.
[18] M. Ferri, K. Papchenko, M. Degli Esposti, G. Tondi, M.G. De Angelis, D. Morselli, P. Fabbri, Fully biobased polyhydroxyalkanoate/tannin films as multifunctional materials for smart food packaging applications, ACS Appl. Mater. Interfaces 15 (2023) 28594–28605, https://doi.org/10.1021/acsami.3c04611.
[19] P. Cataldi, P. Steiner, T. Raine, K. Lin, C. Kocabas, R.J. Young, M. Bissett, I. A. Kinloch, D.G. Papageorgiou, Multifunctional biocomposites based on polyhydroxyalkanoate and graphene/carbon nanofiber hybrids for electrical and thermal applications, ACS Appl. Polym. Mater. 2 (2020) 3525–3534, https://doi.org/10.1021/ACSAPM.0C00539.
[20] K. Papchenko, M. Degli Esposti, M. Minelli, P. Fabbri, D. Morselli, M.G. De Angelis, New sustainable routes for gas separation membranes: the properties of poly (hydroxybutyrate-co-hydroxyvalerate) cast from green solvents, J. Memb. Sci. 660 (2022) 120847, https://doi.org/10.1016/J.MEMSCI.2022.120847.
[21] G. Sarapajevaite, K. Baltakys, M. Degli Esposti, D. Morselli, P. Fabbri, Sustainable PHBV/CuS composite obtained from waste valorization for wastewater purification by visible light-activated photocatalytic activity, Adv. Sustain Syst. 7 (2023), https://doi.org/10.1002/adsu.202300112.
[22] A. Raucci, A. Miglione, L. Lenzi, P. Fabbri, J. Di Tocco, C. Massaroni, D.Lo Presti, E. Schena, V. Pifferi, L. Falciola, W. Aidli, C. Di Natale, P.A. Netti, S.L. Woo, D. Morselli, S. Cinti, Characterization and application of porous PHBV-based bacterial polymers to realize novel bio-based electroanalytical (bio)sensors, Sens. Actuators B Chem. 379 (2023) 133178, https://doi.org/10.1016/J.SNB.2022.133178.
[23] T.S.M. Amelia, S. Govindasamy, A.M. Tamothran, S. Vigneswari, K. Bhubalan, Applications of PHA in agriculture, Biotechnol. Appl. Polyhydroxyalkanoates (2019) 347–361, https://doi.org/10.1007/978-981-13-3759-8_13.

[24] A. Pandey, N. Adama, K. Adjallé, J.F. Blais, Sustainable applications of polyhydroxyalkanoates in various fields: a critical review, Int J. Biol. Macromol. 221 (2022) 1184–1201, https://doi.org/10.1016/J.IJBIOMAC.2022.09.098.
[25] C.R. Álvarez-Chávez, S. Edwards, R. Moure-Eraso, K. Geiser, Sustainability of bio-based plastics: general comparative analysis and recommendations for improvement, J. Clean. Prod. 23 (2012) 47–56, https://doi.org/10.1016/J.JCLEPRO.2011.10.003.
[26] J.K. Hobbs, T.J. Mcmaster, M.J. Miles, P.J. Barham, Cracking in spherulites of poly (hydroxybutyrate), Polymers 37 (1996) 3241–3246, https://doi.org/10.1016/0032-3861(96)88468-0.
[27] Z. Špitalský, I. Lacík, E. Lathová, I. Janigová, I. Chodák, Controlled degradation of polyhydroxybutyrate via alcoholysis with ethylene glycol or glycerol, Polym. Degrad. Stab. 91 (2006) 856–861, https://doi.org/10.1016/J.POLYMDEGRADSTAB.2005.06.019.
[28] W.M. Pachekoski, C. Dalmolin, J.A.M. Agnelli, The influence of the industrial processing on the degradation of poly(hidroxybutyrate) - PHB, Mater. Res. 16 (2013) 237–332, https://doi.org/10.1590/S1516-14392012005000180.
[29] A. El-Hadi, R. Schnabel, E. Straube, G. Müller, M. Riemschneider, Effect of melt processing on crystallization behavior and rheology of poly(3-hydroxybutyrate) (PHB) and its blends, Macromol. Mater. Eng. 287 (2002) 363–372, https://doi.org/10.1002/1439-2054.
[30] E. Hablot, P. Bordes, E. Pollet, L. Avérous, Thermal and thermo-mechanical degradation of poly(3-hydroxybutyrate)-based multiphase systems, Polym. Degrad. Stab. 93 (2008) 413–421, https://doi.org/10.1016/J.POLYMDEGRADSTAB.2007.11.018.
[31] R.C. Baltieri, L.H.I. Mei, J. Bartoli, Study of the influence of plasticizers on the thermal and mechanical properties of Poly(3-hydroxybutyrate) compounds, : Macromol. Symp. (2003) 33–44, https://doi.org/10.1002/masy.200350704.
[32] M. Rahman, C.S. Brazel, The plasticizer market: an assessment of traditional plasticizers and research trends to meet new challenges, Prog. Polym. Sci. 29 (2004) 1223–1248, https://doi.org/10.1016/J.PROGPOLYMSCI.2004.10.001.
[33] D.W. Gao, Z.D. Wen, Phthalate esters in the environment: A critical review of their occurrence, biodegradation, and removal during wastewater treatment processes, Sci. Total Environ. 541 (2016) 986–1001, https://doi.org/10.1016/J.SCITOTENV.2015.09.148.
[34] S.S. Muobom, A.-M. Saleem Umar, Y. Soongseok, A.-P. Brolin, A review on plasticizers and eco-friendly bioplasticizers: biomass sources and market, Int. J. Eng. Res. Technol. (IJERT) 9 (2020) 1138–1144, https://doi.org/10.17577/IJERTV9IS050788.
[35] Y.C. Wang, H.S. Chen, C.Y. Long, C.F. Tsai, T.H. Hsieh, C.Y. Hsu, E.M. Tsai, Possible mechanism of phthalates-induced tumorigenesis, Kaohsiung J. Med Sci. 28 (2012), https://doi.org/10.1016/J.KJMS.2012.05.006.
[36] M.G.A. Vieira, M.A. Da Silva, L.O. Dos Santos, M.M. Beppu, Natural-based plasticizers and biopolymer films: a review, Eur. Polym. J. 47 (2011) 254–263, https://doi.org/10.1016/J.EURPOLYMJ.2010.12.011.
[37] A. Sinisi, M. Degli Esposti, S. Braccini, F. Chiellini, S. Guzman-Puyol, J.A. Heredia-Guerrero, D. Morselli, P. Fabbri, Levulinic acid-based bioplasticizers: a facile approach to enhance the thermal and mechanical properties of polyhydroxyalkanoates, Mater. Adv. 2 (2021) 7869–7880, https://doi.org/10.1039/D1MA00833A.
[38] W. Xuan, M. Hakkarainen, K. Odelius, Levulinic acid as a versatile building block for plasticizer design, ACS Sustain Chem. Eng. 7 (2019) 12552–12562, https://doi.org/10.1021/ACSSUSCHEMENG.9B02439.
[39] A. Sinisi, M. Degli Esposti, M. Toselli, D. Morselli, P. Fabbri, Biobased ketal-diester additives derived from levulinic acid: synthesis and effect on the thermal stability and thermo-mechanical properties of poly(vinyl chloride), ACS Sustain Chem. Eng. 7 (2019) 13920–13931, https://doi.org/10.1021/ACSSUSCHEMENG.9B02177.
[40] M. Râpă, R.N. Darie-Nita, E. Matei, A.M. Predescu. Bio-Based Plasticizers for Polyvinylchloride(PVC), 2022, pp. 137–157, 10.1007/978-3-030-78455-3_7.
[41] M. Bocqué, C. Voirin, V. Lapinte, S. Caillol, J.J. Robin, Petro-based and bio-based plasticizers: Chemical structures to plasticizing properties, J. Polym. Sci. A Polym. Chem. 54 (2016) 11–33, https://doi.org/10.1002/POLA.27917.
[42] H. Tan, L. Yang, X. Liang, D. Huang, X. Qiao, Q. Dai, D. Chen, Z. Cai, Nonphthalate plasticizers in house dust from multiple countries: an increasing threat to humans, Environ. Sci. Technol. 57 (2023) 3634–3644, https://doi.org/10.1021/ACS.EST.2C08110.
[43] V. Jost, H.C. Langowski, Effect of different plasticisers on the mechanical and barrier properties of extruded cast PHBV films, Eur. Polym. J. 68 (2015) 302–312, https://doi.org/10.1016/J.EURPOLYMJ.2015.04.012.
[44] E. Campioli, S. Lee, M. Lau, L. Marques, V. Papadopoulos, Effect of prenatal DINCH plasticizer exposure on rat offspring testicular function and metabolism, Sci. Rep. (2017) 1–14, https://doi.org/10.1038/s41598-017-11325-7.
[45] T.T. Bui, G. Giovanoulis, A.P. Cousins, J. Magnér, I.T. Cousins, C.A. de Wit, Human exposure, hazard and risk of alternative plasticizers to phthalate esters, Sci. Total Environ. 541 (2016) 451–467, https://doi.org/10.1016/J.SCITOTENV.2015.09.036.
[46] H.M. Koch, A. Schütze, C. Pälmke, J. Angerer, T. Brüning, Metabolism of the plasticizer and phthalate substitute diisononyl- cyclohexane-1,2-dicarboxylate (DINCH®) in humans after single oral doses, Arch. Toxicol. 87 (2013) 799–806, https://doi.org/10.1007/S00204-012-0990-4.
[47] A. Schütze, M. Lorber, K. Gawrych, M. Kolossa-Gehring, P. Apel, T. Brüning, H. M. Koch, Development of a multi-compartment pharmacokinetic model to characterize the exposure to Hexamoll® DINCH®, Chemosphere 128 (2015) 216–224, https://doi.org/10.1016/J.CHEMOSPHERE.2015.01.056.
[48] W. Zhang, J. Jie, Q. Xu, R. Wei, X. Liao, D. Zhang, Y. Zhang, J. Zhang, G. Su, Y. Chen, D. Weng, Characterizing the obesogenic and fatty liver-inducing effects of Acetyl tributyl citrate (ATBC) plasticizer using both in vivo and in vitro models, J. Hazard. Mater. 445 (2023), https://doi.org/10.1016/J.JHAZMAT.2022.130548.
[49] M. Finkelstein, H. Gold, Toxicology of the citric acid esters: tributyl citrate, acetyl tributyl citrate, triethyl citrate, and acetyl triethyl citrate, Toxicol. Appl. Pharm. 1 (1959) 283–298, https://doi.org/10.1016/0041-008X(59)90113-9.
[50] K. Nara, K. Nishiyama, H. Natsugari, A. Takeshita, H. Takahashi, Leaching of the Plasticizer, Acetyl Tributyl Citrate: (ATBC) from Plastic Kitchen Wrap, J. Health Sci. 55 (2009) 281–284, https://doi.org/10.1248/JHS.55.281.
[51] P.D. Zygoura, K.A. Riganakos, M.G. Kontominas, Study of the migration behavior of acetyl tributyl citrate from PVDC/PVC film into fish fillets as affected by intermediate doses of electron beam radiation, Eur. Food Res. Technol. 232 (2011) 1017–1025, https://doi.org/10.1007/S00217-011-1475-Z.
[52] A. Qadeer, K.L. Kirsten, Z. Ajmal, X. Jiang, X. Zhao, Alternative plasticizers as emerging global environmental and health threat: another regrettable substitution? Environ. Sci. Technol. 56 (2022) 1482–1488, https://doi.org/10.1021/acs.est.1c08365.
[53] A. Giubilini, F. Bondioli, M. Messori, G. Nyström, G. Siqueira, Advantages of additive manufacturing for biomedical applications of polyhydroxyalkanoates, Bioengineering 8 (2021) 1–31, https://doi.org/10.3390/bioengineering8020029.
[54] R.A. Rebia, N.S.B. Sadon, T. Tanaka, Natural antibacterial reagents (Centella, propolis, and hinokitiol) loaded into poly[(R)-3-hydroxybutyrate-co-(R)-3-hydroxyhexanoate] composite nanofibers for biomedical applications, Nanomaterials 9 (2019), https://doi.org/10.3390/nano9121665.
[55] G. Barouti, C.G. Jaffredo, S.M. Guillaume, Advances in drug delivery systems based on synthetic poly(hydroxybutyrate) (co)polymers, Prog. Polym. Sci. 73 (2017) 1–31, https://doi.org/10.1016/J.PROGPOLYMSCI.2017.05.002.
[56] A. Giubilini, G. Siqueira, F.J. Clemens, C. Sciancalepore, M. Messori, G. Nyström, F. Bondioli, 3D-PRinting Nanocellulose-poly(3-hydroxybutyrate- Co-3-hydroxyhexanoate) Biodegradable Composites by Fused Deposition Modeling, ACS Sustain Chem. Eng. 8 (2020) 10292–10302, https://doi.org/10.1021/acssuschemeng.0c03385.
[57] C. De Maria, I. Chiesa, D. Morselli, M.R. Ceccarini, S. Bittolo Bon, M. Degli Esposti, P. Fabbri, A. Morabito, T. Beccari, L. Valentini, Biomimetic tendrils by four dimensional printing bimorph springs with torsion and contraction properties based on bio-compatible graphene/silk fibroin and poly(3-Hydroxybutyrate-co-3-Hydroxyvalerate), Adv. Funct. Mater. 31 (2021) 2105665, https://doi.org/10.1002/ADFM.202105665.
[58] A.S. Alagoz, V. Hasirci, 3D printing of polymeric tissue engineering scaffolds using open-source fused deposition modeling, Emergent Mater. 3 (2020) 429–439, https://doi.org/10.1007/S42247-019-00048-2.
[59] L.X. Lü, Y.Y. Wang, X. Mao, Z.D. Xiao, N.P. Huang, The effects of PHBV electrospun fibers with different diameters and orientations on growth behavior of bone-marrow-derived mesenchymal stem cells, Biomed. Mater. 7 (2012) 015002 https://doi.org/10.1088/1748-6041/7/1/015002.
[60] E.I. Paşcu, J. Stokes, G.B. McGuinness, Electrospun composites of PHBV, silk fibroin and nano-hydroxyapatite for bone tissue engineering, Mater. Sci. Eng.: C 33 (2013) 4905–4916, https://doi.org/10.1016/J.MSEC.2013.08.012.
[61] Ł. Kaniuk, U. Stachewicz, Development and advantages of biodegradable PHA POlymers Based on Electrospun Phbv Fibers for Tissue Engineering and Other Biomedical Applications, ACS Biomater. Sci. Eng. 7 (2021) 5339–5362, https://doi.org/10.1021/acsbiomaterials.1c00757.
[62] T.F. Pereira, M.F. Oliveira, I.A. Maia, J.V.L. Silva, M.F. Costa, R.M.S.M. Thiré, 3D printing of poly(3-hydroxybutyrate) porous structures using selective laser sintering, Macromol. Symp. (2012) 64–73, https://doi.org/10.1002/masy.201100237.
[63] S.R. Subramaniam, M. Samykano, S.K. Selvamani, W.K. Ngui, K. Kadirgama, K. Sudhakar, M.S. Idris, 3D printing: overview of PLA progress, AIP Conf. Proc. 2059 (2019), https://doi.org/10.1063/1.5085958/790435.
[64] W. Kanabenja, K. Passarapark, T. Subchokpool, N. Nawaaukkaratharnant, A. J. Román, T.A. Osswald, C. Aumnate, P. Potiyaraj, 3D printing filaments from plasticized polyhydroxybutyrate/polylactic acid blends reinforced with hydroxyapatite, Addit. Manuf. 59 (2022) 103130, https://doi.org/10.1016/J.ADDMA.2022.103130.
[65] V. Melčová, K. Svoradová, P. Menčík, S. Kontárová, M. Rampichová, V. Hedvičáková, V. Sovková, R. Přikryl, L. Vojtová, FDM 3D printed composites for bone tissue engineering based on plasticized poly(3-hydroxybutyrate)/poly(d,l-lactide) blends, Polymers (2020) 2806, https://doi.org/10.3390/POLYM12122806.
[66] Plasticizers Market Size, Share, Trends, Opportunities & Forecast, (n.d.). https://www.verifiedmarketresearch.com/product/plasticizers-market/ (accessed May 2024).
[67] S. Pierucci, J.J. Klemeš, L. Piazza, S. Bakalis, A.M. Gamba, J.S. Fonseca, D. A. Méndez, A. Viloria, D. Fajardo, N.C. Moreno, I.O. Cabeza, Assessment of different plasticizer-polyhydroxyalkanoate mixtures to obtain biodegradable polymeric films, Chem. Eng. Trans. 57 (2017), https://doi.org/10.3303/CET1757228.
[68] J.L. Audic, L. Lemiègre, Y.M. Corre, Thermal and mechanical properties of a polyhydroxyalkanoate plasticized with biobased epoxidized broccoli oil, J. Appl. Polym. Sci. 131 (2014) 39983, https://doi.org/10.1002/APP.39983.
[69] L. Lenzi, M. Degli Esposti, S. Braccini, C. Siracusa, F. Quartinello, G.M. Guebitz, D. Puppi, D. Morselli, P. Fabbri, Further step in the transition from conventional plasticizers to versatile bioplasticizers obtained by the valorization of levulinic acid and glycerol, ACS Sustain Chem. Eng. 11 (2023) 9455–9469, https://doi.org/10.1021/acssuschemeng.3c01536.

[70] V. Kumar, R. Sehgal, R. Gupta, Blends and composites of polyhydroxyalkanoates (PHAs) and their applications, Eur. Polym. J. 161 (2021), https://doi.org/10.1016/j.eurpolymj.2021.110824.
[71] A. Ashori, M. Jonoobi, N. Ayrilmis, A. Shahreki, M.A. Fashapoyeh, Preparation and characterization of polyhydroxybutyrate-co-valerate (PHBV) as green composites using nano reinforcements, Int J. Biol. Macromol. 136 (2019) 1119–1124, https://doi.org/10.1016/j.ijbiomac.2019.06.181.
[72] Y.K. Dasan, A.H. Bhat, F. Ahmad, Polymer blend of PLA/PHBV based bionanocomposites reinforced with nanocrystalline cellulose for potential application as packaging material, Carbohydr. Polym. 157 (2017) 1323–1332, https://doi.org/10.1016/J.CARBPOL.2016.11.012.
[73] M. Baiardo, G. Frisoni, M. Scandola, M. Rimelen, D. Lips, K. Ruffieux, E. Wintermantel, Thermal and mechanical properties of plasticized poly(L-lactic acid), J. Appl. Polym. Sci. 90 (2003) 1731–1738, https://doi.org/10.1002/APP.12549.
[74] Y. Farrag, B. Montero, M. Rico, L. Barral, R. Bouza, Preparation and characterization of nano and micro particles of poly(3-hydroxybutyrate-co-3-hydroxyvalerate) (PHBV) via emulsification/solvent evaporation and nanoprecipitation techniques, J. Nanopart. Res. 20 (2018) 1–17, https://doi.org/10.1007/S11051-018-4177-7.
[75] L. Hassaini, M. Kaci, N. Touati, I. Pillin, A. Kervoelen, S. Bruzaud, Valorization of olive husk flour as a filler for biocomposites based on poly(3-hydroxybutyrate-co-3-hydroxyvalerate): Effects of silane treatment, Polym. Test. 59 (2017) 430–440, https://doi.org/10.1016/J.POLYMERTESTING.2017.03.004.
[76] J.L. Barbosa, G.B. Perin, M.I. Felisberti, Plasticization of Poly(3-hydroxybutyrate-co-3-hydroxyvalerate) with an oligomeric polyester: miscibility and effect of the microstructure and plasticizer distribution on thermal and mechanical properties, ACS Omega 6 (2021) 3278–3290, https://doi.org/10.1021/ACSOMEGA.0C05765.
[77] N.S. Yatigala, D.S. Bajwa, S.G. Bajwa, Compatibilization improves physico-mechanical properties of biodegradable biobased polymer composites, Compos Part A Appl. Sci. Manuf. 107 (2018) 315–325, https://doi.org/10.1016/J.COMPOSITESA.2018.01.011.
[78] L. Martino, M.A. Berthet, H. Angellier-Coussy, N. Gontard, Understanding external plasticization of melt extruded PHBV–wheat straw fibers biodegradable composites for food packaging, J. Appl. Polym. Sci. 132 (2015) 41611, https://doi.org/10.1002/APP.41611.
[79] A. Kirkpatrick, Some relations between molecular structure and plasticizing effect, J. Appl. Phys. 11 (1940) 255–261, https://doi.org/10.1063/1.1712768.
[80] S. Vita, R. Ricotti, C. Malegori, P. Oliveri, M. Castellano, S. Vicini, Univariate and multivariate strategies for the rheological tests evaluation: Influence of additives in composite materials, J. Appl. Polym. Sci. 137 (2020), https://doi.org/10.1002/APP.49019.
[81] C.Y. Khor, Z.M. Ariff, F.C. Ani, M.A. Mujeebu, M.K. Abdullah, M.Z. Abdullah, M. A. Joseph, Three-dimensional numerical and experimental investigations on polymer rheology in meso-scale injection molding, Int. Commun. Heat Mass Transf. 37 (2010) 131–139, https://doi.org/10.1016/J.ICHEATMASSTRANSFER.2009.08.011.
[82] K.C. Feng, A. Pinkas-Sarafova, V. Ricotta, M. Cuiffo, L. Zhang, Y. Guo, C.C. Chang, G.P. Halada, M. Simon, M. Rafailovich, The influence of roughness on stem cell differentiation using 3D printed polylactic acid scaffolds, Soft Matter 14 (2018) 9838–9846, https://doi.org/10.1039/C8SM01797B.
[83] M.D. Torres, B. Hallmark, D.I. Wilson, Effect of concentration on shear and extensional rheology of guar gum solutions, Food Hydrocoll. 40 (2014) 85–95, https://doi.org/10.1016/J.FOODHYD.2014.02.011.
[84] M. Scandola, M. Pizzofi, G. Ceccorulli, A. Cesiro, S. Paoletti, L. Navarini, Viscoelastic and thermal properties of bacterial poly(D-(-)-fl-hydroxybutyrate), Int J. Biol. Macromol. 10 (1988) 373–377, https://doi.org/10.1016/0141-8130(88)90032-3.
[85] O. Gallot-Lavallée, L. Heux, Dielectric spectroscopy on a PHBV bio-polymer, in: Annual Report - Conference on Electrical Insulation and Dielectric Phenomena, CEIDP, 2013, pp. 559–562, https://doi.org/10.1109/CEIDP.2013.6748275.
[86] A. Alhanish, M.A. Ghalia, Developments of biobased plasticizers for compostable polymers in the green packaging applications: a review, Biotechnol. Prog. 37 (2021) e3210, https://doi.org/10.1002/BTPR.3210.
[87] Z.W. Ren, Z.Y. Wang, Y.W. Ding, J.W. Dao, H.R. Li, X. Ma, X.Y. Yang, Z.Q. Zhou, J. X. Liu, C.H. Mi, Z.C. Gao, H. Pei, D.X. Wei, Polyhydroxyalkanoates: the natural biopolyester for future medical innovations, Biomater. Sci. 11 (2023) 6013–6034, https://doi.org/10.1039/D3BM01043K.
[88] A.L. Rivera-Briso, Á. Serrano-Aroca, Poly(3-Hydroxybutyrate-co-3-Hydroxyvalerate): enhancement strategies for advanced applications, Polym. (Basel) 10 (2018), https://doi.org/10.3390/polym10070732.
[89] C. Sciancalepore, E. Togliatti, M. Marozzi, F.M.A. Rizzi, D. Pugliese, A. Cavazza, O. Pitirollo, M. Grimaldi, D. Milanese, Flexible PBAT-based composite filaments for tunable FDM 3D printing, ACS Appl. Biol. Mater. 5 (2022) 3219–3229, https://doi.org/10.1021/acsabm.2c00203.
[90] M. Degli Esposti, M. Changizi, R. Salvatori, L. Chiarini, V. Cannillo, D. Morselli, P. Fabbri, Comparative study on bioactive filler/biopolymer scaffolds for potential application in supporting bone tissue regeneration, ACS Appl. Polym. Mater. 4 (2022) 4306–4318, https://doi.org/10.1021/acsapm.2c00270.
[91] N. Abbasi, S. Hamlet, R.M. Love, N.T. Nguyen, Porous scaffolds for bone regeneration, J. Sci.: Adv. Mater. Devices 5 (2020) 1–9, https://doi.org/10.1016/J.JSAMD.2020.01.007.
[92] S. Nguyen, G.E. Yu, R.H. Marchessault, Thermal degradation of poly(3-hydroxyalkanoates): Preparation of well-defined oligomers, Biomacromolecules 3 (2002) 219–224, https://doi.org/10.1021/BM0156274.
[93] M. Kunioka, Y. Doi, Thermal degradation of microbial copolyesters: Poly(3-hydroxybutyrate-co-3-hydroxyvalerate) and Poly(3-hydroxybutyrate-co-4-hydroxybutyrate), Macromolecules 23 (1990) 1933–1936, https://doi.org/10.1021/MA00209A009.
[94] J. Lim, M. You, J. Li, Z. Li, Emerging bone tissue engineering via Polyhydroxyalkanoate (PHA)-based scaffolds, Mater. Sci. Eng. C 79 (2017) 917–929, https://doi.org/10.1016/j.msec.2017.05.132.
[95] L.M.W.K. Gunaratne, R.A. Shanks, G. Amarasinghe, Thermal history effects on crystallisation and melting of poly(3-hydroxybutyrate), Thermochim. Acta 423 (2004) 127–135, https://doi.org/10.1016/J.TCA.2004.05.003.
[96] A. Giubilini, C. Sciancalepore, M. Messori, F. Bondioli, New biocomposite obtained using poly(3-hydroxybutyrate-co-3-hydroxyhexanoate) (PHBH) and microfibrillated cellulose, J. Appl. Polym. Sci. 137 (2020) 48953, https://doi.org/10.1002/APP.48953.
[97] K. Yasuda, R.C. Armstrong, R.E. Cohen, Shear flow properties of concentrated solutions of linear and star branched polystyrenes, Rheol. Acta 20 (1981) 163–178, https://doi.org/10.1007/BF01513059.
[98] E. Togliatti, D. Milanese, D. Pugliese, C. Sciancalepore, Viscoelastic characterization and degradation stability investigation of poly(butylene-adipate-co-terephthalate) – calcium-phosphate glass composites, J. Polym. Environ. 30 (2022) 3914–3933, https://doi.org/10.1007/s10924-022-02479-1.
[99] C. Sciancalepore, E. Togliatti, A. Giubilini, D. Pugliese, F. Moroni, M. Messori, D. Milanese, Preparation and characterization of innovative poly(butylene adipate terephthalate)-based biocomposites for agri-food packaging application, J. Appl. Polym. Sci. (2022) 52370, https://doi.org/10.1002/app.52370.